Stresses developed during clinical debonding of stainless steel orthodontic brackets

Thomas R. Katona, PhD, DMD

Orthodontic bracket debonding often presents clinical challenges. For example, fracture location is an important factor when considering chair time and potential damage to the pulp and enamel surface. If cement residue remains on the enamel, finishing procedures are required. This engenders risks to the tooth. However, debonding techniques that tend to produce "clean" separation at the enamel interface are more likely to cause enamel fracture.[1,2] Since it is the mechanical environment that governs debonding and many of the related iatrogenic complications, the purpose of this project was to examine the stresses generated during five different debonding procedures.

Numerous articles have been devoted to experimental studies of debonding methods[1,3-7] and there are many more that deal with the laboratory determination of direct bonded orthodontic bracket strength.[8-12] In the latter, frequently addressed variables include cement type, bracket design, placement technique, and test loading mode. In other investigations,[13,14] finite element modeling (FEM) has been used to calculate the stress field distributions developed during the strength testing protocols. For this project, that FEM approach has been adapted to investigate the peak stresses produced during debonding,

Abstract

The purpose of this project was to use finite element modeling to calculate and compare the peak stresses generated during clinical debonding of resin bonded brackets. Five debonding techniques were considered: tension, shear-peel, torsion loads on the bracket, wedging of the cement margin, and bracket temperature increase. The data is presented in terms of the relative potentials of the methods for causing enamel fracture. That is, in this idealized model, it was assumed that enamel failures were governed by maximum principal or shear stress. Therefore, all debonding loads and calculated stresses were scaled to correspond to unit peak principal stress or unit peak shear stress in enamel. Furthermore, it was assumed that cement cohesive failure was also governed by maximum principal or maximum shear stress and that adhesive failures were caused by interface normal or shear stress. Thus, for example, it was found that for 1.0 MPa of peak shear stress in enamel, tension and shear-peel debonding generate, respectively, 1.34 and 0.96 MPa of peak normal (tensile) stress in the cement at the enamel-cement interface. The interpretation of this information is that tension debonding is less likely to cause enamel damage than shear-peel loading if it is assumed that (1) the enamel would fail due to the high shear stress, and (2) the joint would fail at the enamel-cement interface because its normal stress limit has been exceeded.

Key Words

Orthodontic brackets • Debonding • Dental stress analysis

Submitted: May 1995 **Accepted for publication:** November 1995 Angle Orthod 1997;67(1):39-46.

Table 1
Assumed failure associated mechanical components

Enamel	Enamel-cement interface	Cement-bracket interface	Cement
MAX	ZZ	ZZ	MAX
SHR	XY	XY	SHR

Table 2
Material property approximations[13,16]

	Enamel	Cement	SS bracket
Young's Modulus (MPa)	5.0×10^4	5.0×10^3	2.0×10^5
Poisson's Ratio	0.30	0.38	0.27
Coefficient of thermal expansion ($^oC^{-1}$)			18.0×10^{-6}

with an emphasis on enamel fracture.

In general, the goal of experimental strength testing is to determine the ultimate strength of the joint. The modeling of that process requires examination of the enamel-cement and bracket-cement interface stresses and the stresses within the cement. For the study of debonding, emphasis must also be placed on the stresses within enamel, i.e., the causes of enamel fracture. Thus, the stresses in cement and enamel produced by five debonding techniques used with stainless steel brackets were calculated.

Materials and methods

Relatively little is known about the failure of enamel and cements. For example, it is not clear what stress component causes enamel damage or what stress may be responsible for interface separation. Therefore, for the purposes of this analysis, several failure criteria were considered (Table 1). For simplicity, it was assumed that enamel fracture and cement (cohesive) failure may be initiated by high principal tensile (MAX) or maximum shear (SHR) stress when their respective strengths are exceeded. It was also assumed that interface bonding was complete and that enamel-cement (EC) and cement-bracket (CB) interface (adhesive) failures were governed by interface normal (ZZ) or in plane shear (XY) stress. Failure of the stainless steel brackets was not examined. (A study of ceramic bracket debonding would also require bracket failure considerations.)

The converged three-dimensional FE model (Figure 1) used to calculate the stresses consisted of 21,217 nodes and 18,496 elements. Model generation and postprocessing were done with Patran (PDA Engineering, Costa Mesa, Calif), while analysis was performed with Abaqus (Hibbit, Karlsson, and Sorensen, Inc, Providence, R.I.). Bracket base dimensions approximated the size of a flattened standard clinical bracket. The enamel, whose top surface was also flattened, was fixed on its bottom surface. Loads were applied to simulate the debonding methods. The "active set" feature of the software was implemented to accommodate material property discontinuities (Table 2) across interfaces. All materials were assumed to be homogeneous, isotropic, and linearly elastic.

All debonding force magnitudes, temperature change, and all corresponding calculated stress components were scaled to yield a maximum value of MAX in enamel (MAXe) equal to 1.0 MPa. Similar scaling computations were performed to obtain 1.0 MPa for the maximum magnitude of SHR in enamel (SHRe). (For simplicity, thermal debonding was modeled by a uniform increase in the temperature of the bracket superstructure).

The normalization of stresses relative to unit stresses within enamel made it possible to compare the debonding techniques. In effect, therefore, the comparisons are based on the potential of each debonding method to cause enamel fracture.

Results

For purposes of presentation, the MAXe = 1.0 MPa condition is used as the standard. Thus, the results shown in Table 3A are expressed in terms of MAXe = 1.0 MPa. For example, to generate 1.0 MPa of SHRe, a 5.62 N tensile force must be applied to the bracket. In turn, that load produces maximum ZZ = 1.06 x 1.26 = 1.34 MPa, maximum XY = 0.15 x 1.26 = 0.19 MPa at EC, maximum MAX = 1.11 x 1.26 = 1.40 MPa within the cement, and so on.

Compared with the 5.62 N tension loading (see above), a 6.62 N debonding shear force must be applied to produce the same SHRe = 1.0 MPa (Table 3B). But, the corresponding stresses at EC are maximum ZZ = 1.03 x 0.93 = 0.96 MPa (*vs.* 1.34 MPa in tension) and XY = 0.59 x 0.93 = 0.55 MPa (*vs.* 0.19 MPa in tension). Similarly, Tables 3C and D present the results for the torsion and wedging debonding methods. And to produce MAXe = 1.0 MPa, the bracket superstructure temperature must be increased by 2.5°C, Table 3E.

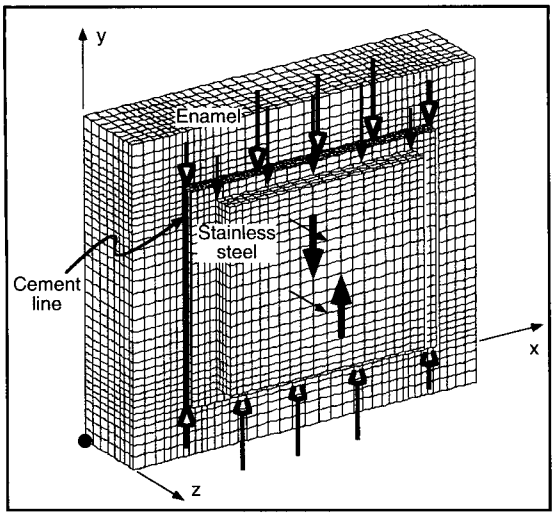

Figure 1A

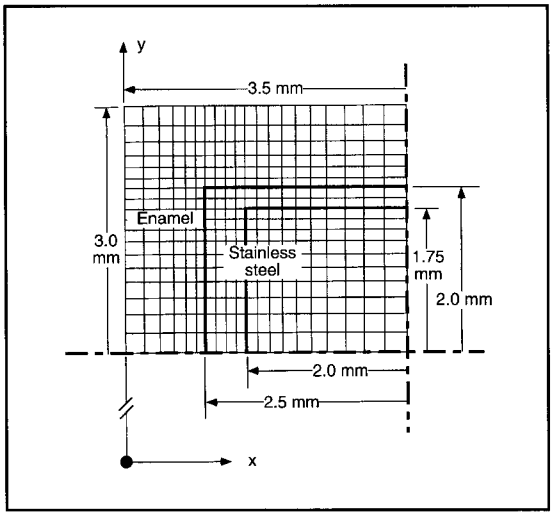

Figure 1B

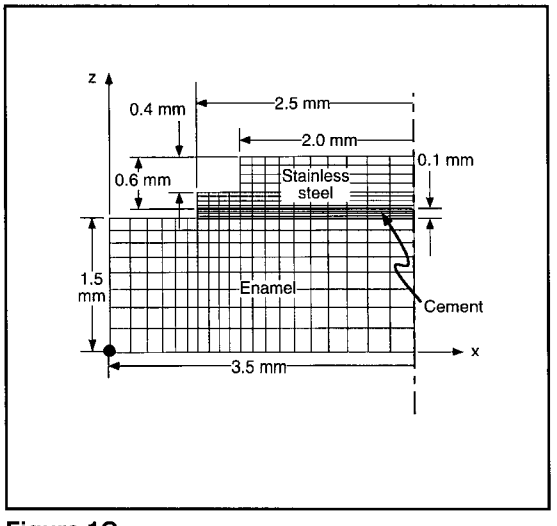

Figure 1C

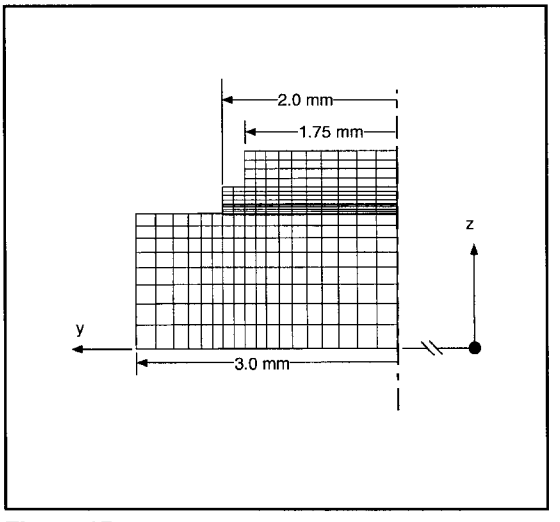

Figure 1D

Figure 1A-D
A: The FEM of the entire structure. The debonding forces act on nodes indicated by the locations of the force vector arrow tips. Tensile debonding load is represented by two thin arrows. Shear-peel debonding is modeled with the five solid arrows at the junction of the base and bracket superstructure. Thick gray vectors provide torsion load, and 10 open arrows, acting at midthickness of the cement, make up the wedging technique. Since there are two planes of structural symmetry, for detail clarity, only a quarter of the assembly is illustrated in the front (B), top (C), and side (D) views. For orientation, black dots locate the origin. Note, since the loading is not symmetric in all methods, the full model, A, was actually solved.

The tabulated results are shown graphically in Figure 2. The information in the top rows of Tables 3A-E (i.e., the MAXe = 1.0 data) is depicted in Figure 2A. All the SHRe = 1.0 results are in Figure 2B. Note that the loading units differ. Traction in tension, shear, and wedging is stated in N. The unit of torsion loading is N-mm, while thermal debonding is expressed by an increase in temperature. Clearly, these variables cannot be compared directly. But, as will be seen in the Discussion, for the purposes of this analysis, the debonding loads themselves are unimportant; what matters are the relative stresses that they produce.

Discussion

Due to the paucity of knowledge about the failure of enamel, cements, and interfaces, calculations were performed for several possible failure modes (Table 1). For all debonding techniques, the maximum values of the stress components listed in Table 1 were determined and normalized relative to the stress components in enamel (Table 3).

The tension, shear-peel, and torque debonding loads were applied directly to the superstructure of the bracket. These are more realistic approximations to clinical procedures than the fourth mechanical method, wedging. In the latter, forces were applied to the center of the cement line thickness. One description of a similar clinical procedure is given as the application of a force with debonding pliers or ligature cutter at the enamel **or** bracket interface.[4] That clinical technique cannot apply the force uniformly across the width of the cement line, and in terms of stress generation, it makes a difference if the force is applied at the enamel or bracket interface. Furthermore, in an earlier study,[3] it was found that the actual force location was difficult to determine.

The FE model of thermal debonding is simplified because it is assumed that the bracket su-

Table 3
The tensile loads on stainless steel brackets required to produce unit maximum values of MAX and SHR in enamel, and the concomitant maximum stress components at the interfaces and within the cement (A). Similarly for shear-peel, torsion, wedge, and thermal debonding, (B), (C), (D), and (E), respectively.

Table 3A

Enamel (MPa)	Required load: Tension (N)	Enamel-cement (MPa)	Cement-bracket (MPa)	Cement (MPa)
MAXe=1.0	4.46	ZZ = 1.06	ZZ = 1.11	MAX = 1.11
		XY = 0.15	XY = 0.11	SHR = 0.56
SHRe=1.0	5.62	Multiply MAXe = 1.0 results by 5.62/4.46 = 1.26		

Table 3B

Enamel (MPa)	Required load: Shear (N)	Enamel-cement (MPa)	Cement-bracket (MPa)	Cement (MPa)
MAXe=1.0	7.14	ZZ = 1.03	ZZ = 0.67	MAX = 1.39
		XY = 0.59	XY = 0.62	SHR = 1.26
SHRe=1.0	6.62	Multiply MAXe = 1.0 results by 6.62/7.14 = 0.93		

Table 3C

Enamel (MPa)	Required load: Torque (N-mm)	Enamel-cement (MPa)	Cement-bracket (MPa)	Cement (MPa)
MAXe=1.0	11.29	ZZ = 0.93	ZZ = 1.01	MAX = 1.21
		XY = 0.50	XY = 0.47	SHR = 1.01
SHRe = 1.0	9.43	Multiply MAXe = 1.0 results by 9.43/11.29 = 0.84		

Table 3D

Enamel (MPa)	Required load: Wedge (N)	Enamel-cement (MPa)	Cement-bracket (MPa)	Cement (MPa)
MAXe = 1.0	1.04	ZZ = 0.40	ZZ = 0.42	MAX = 2.63
		XY = 4.44	XY = 4.28	SHR = 15.1
SHRe = 1.0	0.54	Multiply MAXe = 1.0 results by 0.54/1.04 = 0.52		

Table 3E

Enamel (MPa)	Required: Temp. (+°C)	Enamel-cement (MPa)	Cement-bracket (MPa)	Cement (MPa)
MAXe=1.0	2.51	ZZ = 0.71	ZZ = 0.68	MAX = 0.91
		XY = 0.87	XY = 0.62	SHR = 1.83
SHRe=1.0	2.11	Multiply MAXe = 1.0 results by 2.11/2.51 = 0.84		

perstructure is uniformly heated and that the cement is not affected by heat. A more realistic model would also include thermal conduction, but such complex analysis was deemed unnecessary for the purposes of this early project. It should also be noted that there are other debonding techniques that are not considered herein. These include the squeezing together of wings[3,4] and the simultaneous application of torque to the bracket base and cement.[5]

For an explanation of the results, consider debonding in tension (Table 3A). As the load is applied, the various stress components (ZZ, XY, MAX, and SHR) at the different locations (enamel, EC, CB, and cement) within the structure increase according to the proportions listed in the table. When any of these components exceeds its limit, joint failure occurs. Because most of these limits are not known for the various enamel surface preparations, cement types,

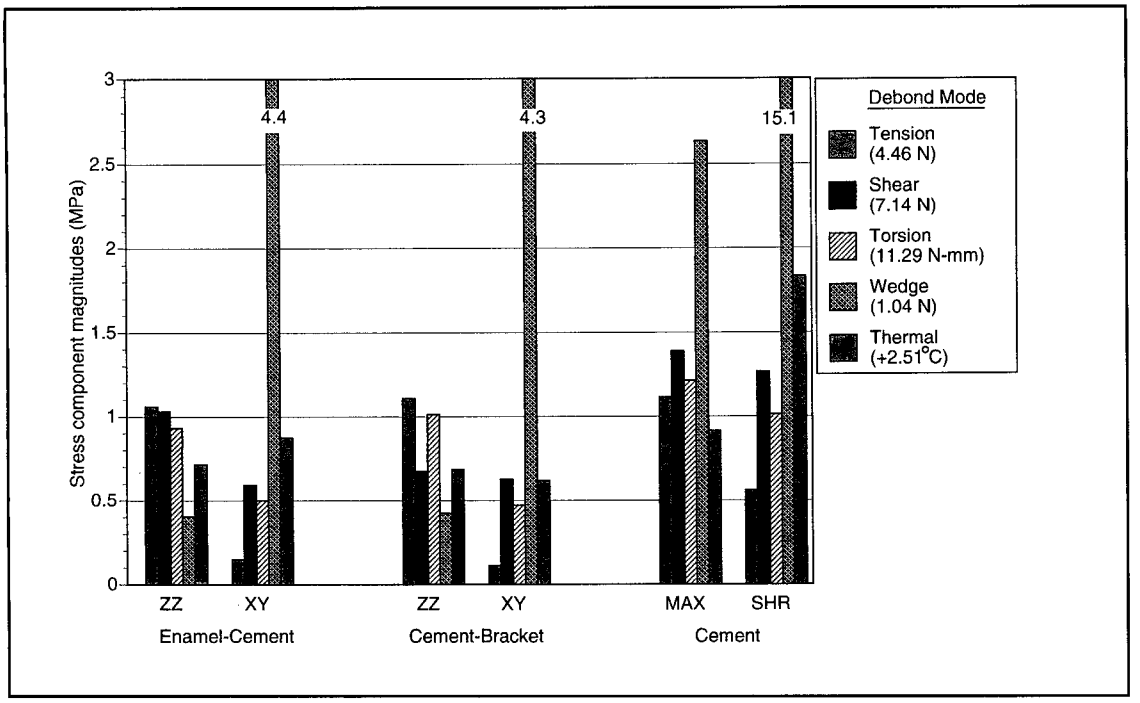

Figure 2A

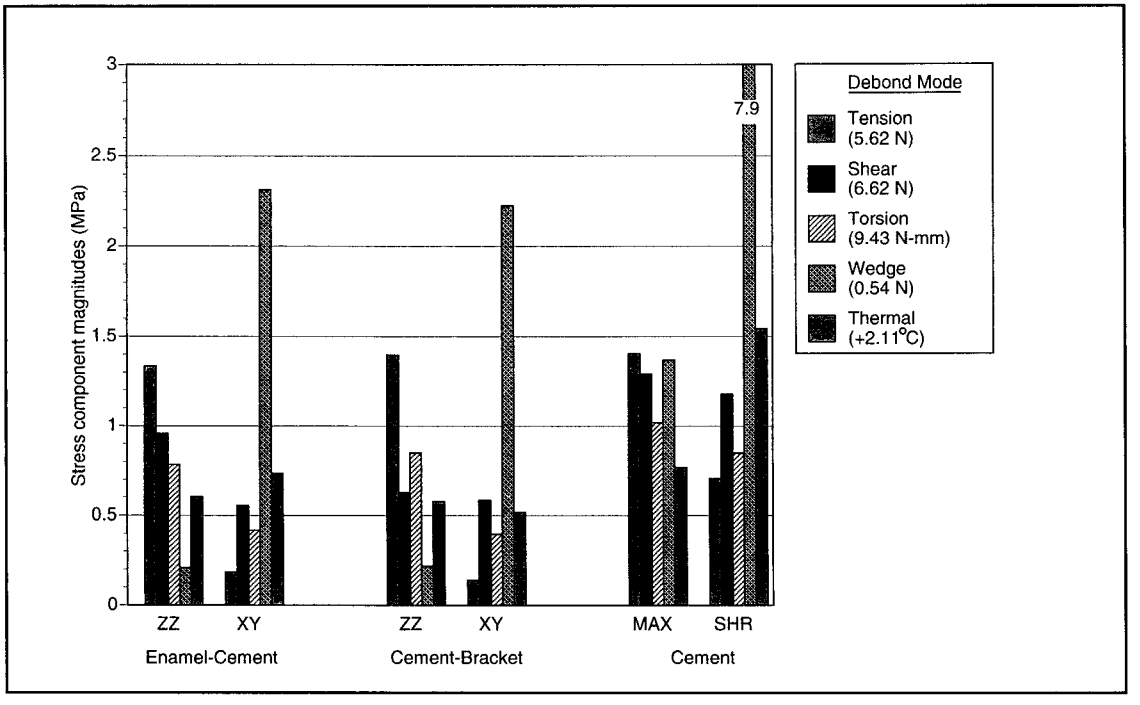

Figure 2B

Figure 2A-B
Stress components.
A: Results are for debond loads that yielded MAXe=1.0 MPa. Graph presents data from top rows of Table 3A-E.
B: Calculations for SHRe=1.0 MPa.

bracket base designs and materials, the results must be considered with a "what if" approach.

Assume, for example, that enamel fracture would take place when MAXe surpasses the tensile strength of enamel. But, that could only happen if no other enamel, interface, or cement stress component reached its respective limit first. If, for example, debonding at CB were governed by the XY component, then enamel fracture could not happen if the ratio of the CB interface shear (XY) strength divided by enamel tensile (MAXe) strength is less than 0.11/1.0 (Table 3A). Note that this condition would be sufficient to protect enamel from failing due to high MAXe (because the CB interface would break first), but it does not necessarily mean that failure would take place at the CB interface. For example, if EC failure is governed by a limit on ZZ, then that interface would fail prior to the CB interface if the ratio of the ZZ limit at EC divided by the CB

shear (XY) strength is less than 1.06/0.11 . Furthermore, it is also theoretically possible that the enamel could fracture due to high SHR if that limit is reached first. However, since the enamel shear strength/tensile strength ratio is approximately 8/1,[15] this is not likely with the debonding methods considered herein. That is because the maximum calculated ratio of SHRe/MAXe (obtained with the wedge debonding method, Table 3D) is only 1.04/0.54 ∪ 2/1 .

Another important observation is that if separation occurs primarily at the bracket,[11,16] it does not necessarily imply that adhesion to enamel is stronger (and conversely). The bracket bond may, in fact, be stronger, but it may have been exposed to higher stresses. And, as shown in this project, the relative stresses at the interfaces depend on the loading mode. For example, in tension, the ZZ component ratio at EC over CB is 1.06/1.11 = 0.95 (Table 3A). In shear-peel, that ratio is 1.03/0.67 = 1.54 (Table 3B). This means that it may be possible for the identical joint to fail at the bracket in tension loading but at the enamel in shear-peel loading. (In this hypothetical situation, it is assumed that the ZZ component at the interfaces governs failure.)

A different perspective of the results is as follows. For an equal likelihood of EC and BC interface shear stress (XY) causing failure in tensile loading, the ratio of their shear bond strengths would have to be 0.15/0.11, Table 3A. If the ratio is higher than that, then failure could not occur at the former (EC) location. With a lower ratio, failure could not occur at the latter (BC). Similarly, for equal normal (ZZ) and shear (XY) stress failure probability at EC, the normal/shear stress bond strength proportionality must be 1.06/0.15 = 7.07, Table 3A. The same reasoning applies to all combinations of stresses shown in Table 3.

Of particular importance for the analysis of enamel fracture is the ratios of the various interface and cement stress components divided by the stress components in enamel. It must be emphasized, again, that the stress ratios depend on the loading mode. For example, in shear loading (Table 3B), the ZZ/XY ratio at EC would be 1.03/0.59 = 1.75 (vs. 7.07 in tension, as shown above).

Since actual stress component failure limits are generally unknown, it is impossible to calculate the necessary levels of loading to cause debonding or to predict the location of failure. To do so would require complete information on the strength limits of the stress components listed in Table 3. With currently available data, such tables would be very sparse. For example, the bulk tensile (MAX) and shear (SHR) strengths of the particular cement, as well as enamel, would be needed. Such information is probably available for some cements, but in addition, its bond strengths (in terms of ZZ and XY) with enamel

and bracket must also be known. These values, in turn, would depend on such factors as enamel surface preparation[17] and bracket base design. Until such information becomes available, these results have limited, but important, implications.

As noted previously, the tables and figures must be interpreted on a "what if" basis. For example, it can be seen in the first sets of five bars in Figures 2A and B that the chance of EC failure due to high ZZ decreases, in order, with tension, shear, torsion, thermal, and wedge debonding. Therefore, the concomitant risk of enamel damage due to MAXe or SHRe increases. In contrast, if MAX in cement was the limiting factor, then the sequence would be wedge, shear, torsion, tension, and thermal loading for MAXe = 1.0 (Fig. 2A), and tension, wedge, shear, torsion, and thermal loading for SHRe = 1.0 (Fig. 2B).

Clearly, it is impractical to discuss the numerous combinations of failure criteria presented herein. The few specific examples serve to illustrate the concepts and the analysis approach. Other important confounding issues that must be considered include material effects. For example, because ceramic brackets have a different Young's modulus and coefficient of thermal expansion than stainless steel, the generated stresses would be different. Furthermore, since the adhesion mechanism is different, not only will the interface strengths be different, but they may be governed by different stress components. Changing the cement would have similar effects.

Conclusions

This basic analysis of an idealized model has shown that orthodontic debonding is a very complex mechanical process. But, as illustrated, FEM based stress analysis could be an exceedingly powerful tool for the prediction of failure and for the development of less iatrogenic debonding techniques. However, to enable this approach to be effective, more experimental strength data must be obtained.

Acknowledgments

The author gratefully acknowledges the assistance provided by Jian Huang. Supported by NIDR grant DE11054.

Author Address

Thomas R. Katona
Indiana University
Purdue University at Indianapolis
School of Dentistry
1121 W. Michigan St
Indianapolis, IN 46202

T.R. Katona, assistant professor, Department of Oral Facial Development, Indiana University School of Dentistry and Department of Mechanical Engineering, Purdue University, Indiana University - Purdue University at Indianapolis.

References

1. Storm ER. Debonding ceramic brackets. J Clin Orthod 1990;24:91-94.
2. Yapel MJ, Quick DC. Experimental traumatic debonding of orthodontic brackets. Angle Orthod 1994;64:131-136.
3. Oliver RG. The effect of different methods of bracket removal on the amount of residual adhesive. Am J Orthod Dentofac Orthop 1988;93:196-200.
4. Kinch AP, Taylor H, Warltier R, Oliver RG, Newcombe RG. A clinical study of amount of adhesive remaining on enamel after debonding, comparing etch times of 15 and 60 seconds. Am J Orthod Dentofac Orthop 1989;95:415-421.
5. Odegaard J. Debonding ceramic brackets. J Clin Orthod 1989;23:632-635.
6. Bishara SE, Fehr DE, Jakobsen JR. A comparative study of the debonding strengths of different ceramic brackets, enamel conditioners, and adhesives. Am J Orthod Dentofac Orthop 1993; 104:170-179.
7. Bishara SE, Fonseca JM, Fehr DE, Boyer DB. Debonding forces applied to ceramic brackets simulating clinical conditions. Angle Orthod 1994;64:277-282.
8. Miles PG, Pontier J-P, Bahiraei D, Close J. The effect of carbamine peroxide bleach on the tensile bond strength of ceramic brackets: An *in vitro* study. Am J Orthod Dentofac Orthop 1994; 106:371-375.
9. McCarthy MF, Hondrum SO. Mechanical and bond strength properties of light-cured and chemically-cured glass ionomer cements. Am J Orthod Dentofac Orthop 1994;105:135-141.
10. Martin S, Garcia-Godoy F. Shear bond strength of orthodontic brackets cemented with a zinc oxide-polyvinyl cement. Am J Orthod Dentofac Orthop 1994;106:615-620.
11. Wiltshire WA. Shear bond strengths of a glass ionomer for direct bonding in orthodontics. Am J Orthod Dentofac Orthop 1994;106:127-130.
12. Merrill SW, Oesterle LJ, Hermesch CB. Ceramic bracket bonding: A comparison of shear, tensile, and torsional bond strengths of ceramic brackets. Am J Orthod Dentofac Orthop 1995;106:290-297.
13. Katona TR, Moore BK. The effects of load misalignment on tensile load testing of direct bonded orthodontic brackets: A finite element model. Am J Orthod Dentofac Orthop 1994;105:543-551.
14. Katona TR. The effects of load location and misalignment on shear/peel testing of direct bonded orthodontic brackets: A finite element model. Am J Orthod Dentofac Orthop 1994;106:395-402.
15. Craig RG, editor. Restorative Dental Materials. St. Louis: CV Mosby, 1989.
16. Cook PA, Youngson CC. An in vitro study of the bond strength of a glass ionomer cement in the direct bonding of orthodontic brackets. Br J Orthod 1988;15:247-253.
17. Katona TR, Batterman SC. Surface roughness effects on the stress analysis of adhesive joints. Int J Adhesion and Adhesives 1983;3:85-91.